ADVANCED FUNCTIONAL MATERIALS
www.afm-journal.de

Rheological and Drying Considerations for Uniformly Gravure-Printed Layers: Towards Large-Area Flexible Organic Light-Emitting Diodes

Gerardo Hernandez-Sosa, Nils Bornemann, Ingo Ringle, Michaela Agari, Edgar Dörsam, Norman Mechau,* and Uli Lemmer*

Printing organic semiconductor inks by means of roll-to-roll compatible techniques will allow a continuous, high-volume fabrication of large-area flexible optoelectronic devices. The gravure printing technique is set to become a widespread process for the high throughput fabrication of functional layers. The gravure printing process of a poly-phenylvinylene derivative light-emitting polymer dissolved in a two solvent mixture on poly(3,4-ethylenedioxythiophene):poly(styrene sulfonate) (PEDOT:PSS) is studied. The surface tensions, contact angles, viscosities, and drying times of the formulations are investigated as a function of the solvent volume fraction and polymer concentration. The properties of the ink grant a homogeneous printed layer, suitable for device fabrication, when the calculated film leveling time is shorter than a critical time, at which the film has been frozen due to loss of solvent via evaporation. The knowledge obtained from the printing process is applied to fabricate organic light-emitting diodes (OLEDs) on flexible substrates, yielding a luminance of ≈5000 cd m^{-2}.

1. Introduction

The full potential of organic electronics can be exploited by combining the solution processability and a wide range of electronic properties of organic functional materials to produce low-cost, large-area efficient optoelectronic applications for use in daily life. However, the wide-spread use of flexible solar panels, large-area flexible displays, smart wallpapers, interactive packaging, etc. can only be attained if the industrial techniques for large scale production are able to yield high performance reproducible devices at a high throughput rate.[1] Research of organic electronics on the laboratory scale is generally focused on spin coating, blade coating, and/or vacuum evaporation, which are the standard processing techniques for the preparation of optoelectronic devices. These approaches have been helpful tools for conceiving a better understanding of the physical principles governing the function of organic light-emitting diodes (OLEDs), organic photovoltaics (OPVs), or organic field-effect transistors (OFETs).[2] For example, OPVs power conversion efficiencies reach nearly 10% and OFETs with carrier mobility within the range of that of amorphous silicon have been recently reported.[3] Nevertheless, these standard device fabrication techniques are usually not compatible with the concept of large-area low-cost applications on an industrial scale.

Since the introduction of the printing press by Gutenberg in the 15th century, the field of graphical printing has developed techniques that allow the transfer of color ink patterns to produce huge volumes of newspapers, magazines, packaging, etc. on a daily basis. Currently, the field of organic electronics is aiming to profit from this knowledge. Printing functional inks by means of roll-to-roll compatible techniques would allow a continuous, high-volume fabrication process of multilayered devices. Among these techniques, gravure printing is set to become a widespread technique for the high throughput fabrication of functional layers on flexible substrates due to its resistance to a wide variety of solvents, high printing speeds (1–10 m s^{-1}), and high lateral resolution on the micrometer scale.[4]

In recent years, gravure printing has been utilized for the fabrication of layers for OLEDs, OFETs, and OPVs with very promising results.[5–7] Nevertheless, the low viscous nature of the functional inks and the small layer thicknesses required for device fabrication (<100 nm for active layers) give raise to problems during the film formation process. It is not uncommon that functional ink formulations yielding high performance devices by spin-coating fail to produce good quality films when

Dr. G. Hernandez-Sosa, Dr. N. Mechau, Prof. U. Lemmer
Light Technology Institute
Karlsruhe Institute of Technology
Engesserstr. 13, 76131 Karlsruhe, Germany
E-mail: gerardo.sosa@kit.edu; norman.mechau@kit.edu
Dr. G. Hernandez-Sosa, Dr. N. Mechau, Prof. U. Lemmer
InnovationLab GmbH, Speyerer Strasse 4, 69115 Heidelberg, Germany
N. Bornemann, Prof. E. Dörsam
Institute for Printing Science and Technology
Technical University Darmstadt
Magdalenenstr. 2, 64289 Darmstadt, Germany
I. Ringle, Dr. M. Agari
Heidelberger Druckmaschinen AG
Kurfürstenanlage 52-60, 69115 Heidelberg, Germany

DOI: 10.1002/adfm.201202862

gravure printed.[6,8] The presence of layer defects often related to poor wetting of the substrate or to surface modulations, arising from hydrodynamic or thin film instabilities, results in a surface topography or interface quality not adequate for device fabrication.[9] The latter can be strongly influenced by changing the rheological properties and drying conditions of the functional ink formulation. Contrary to the case of conventional inks used for graphical printing, the formulation of a functional ink cannot be arbitrarily changed to adjust its fluid properties (e.g., viscosity or surface tension) to achieve a better printability. As it has been shown in literature, the choice of solvent and additives strongly influences the device performance causing morphological changes that ultimately affect the fundamental properties of the active layer (e.g., carrier mobility, efficiency of carrier collection or recombination, etc.).[10] Moreover, the fabrication of multilayered devices, in which the subsequent printing of a dielectric, injection or active layer is needed, implies an additional restriction on the solvent choice to avoid dissolution and intermixing of the previously printed layer. The simplest approach for adjusting the viscosity and surface tension of the functional inks involves changing the solute concentration or using a different solvent (or even a mixture of solvents). Furthermore, surface treatment of the substrate can be used to alter its surface tension and improve its wettability.[11] The recent advances in the fabrication of gravure printed organic electronic devices represent an important and encouraging proof of principle towards the use of this technique as a mass production tool. However, they are only partially devoted to the understanding of the functional ink properties needed to produce thin films adequate for device applications. Chung et al. for example, fabricated high performance OLEDs focusing on optimizing the wettability of the substrate by using different solvent mixtures.[6] However, surface modulations were still present for some formulations even if their properties would allow them to completely wet the substrate. Voigt and collaborators have reported the fabrication of high performance gravure printed OFETs using an organic active layer and dielectric and Ag-ink for the electrodes. In order to identify the best printing conditions, formulations with different solvents were tested and their viscosity characterized.[7] Nevertheless, film inhomogeneities were still present after printing the dielectric layer. For the OLEDs prepared in ref. [8], the authors simply chose to partially dissolve the printed active layer in order to reduce surface roughness. Therefore, in order to contribute to the improvement of the quality, reproducibility, and performance of gravure printed functional films, a better understanding of the optimal ink properties is required.

In this work we study the gravure printing process of the poly-phenylvinylene derivative light emitting polymer colloquially named super yellow (SY) on poly(3,4-ethylenedioxythiophene):poly(styrene sulfonate) (PEDOT:PSS) surfaces and apply the results to the fabrication of flexible OLEDs. SY can be easily dissolved in toluene and has been used in our laboratory to fabricate solution processed OLEDs by spin coating.[12] However, when gravure printed, this formulation yields films with high surface modulation unsuitable for devices. Therefore, in order to prepare SY ink formulations suitable for gravure printing, solvent mixtures formed by toluene and benzothiazole are used. Benzothiazole is a high boiling point solvent (230 °C) and should therefore be expected to delay the drying time of the film contributing to surface demodulation. The viscosity of the formulation is systematically investigated by changing the SY concentration and the volume fraction of the solvents while keeping the surface tension within a suitable window to allow wetting of the substrate. We observe, upon increase of benzothiazole volume fraction that the film drying time increases although favorable film conformation is only permitted within a range of solvent ratios. To explain these results we make use of a model that takes into consideration the viscosity and surface tension of the ink to estimate the surface demodulation time, and compare this value to the drying time of the film. As expected, the rheological properties of the ink will grant a homogeneous printed layer, suitable for device fabrication, when the demodulation time is shorter than a critical time, at which the film has been "frozen" due to loss of solvent via evaporation. In our investigation this condition is accomplished for formulations with compositions where the ink viscosity presents a local minimum and a Newtonian behavior. As a final part of this work, we apply the knowledge obtained from the printing process to fabricate flexible OLEDs with homogenous layers yielding a luminance of ≈5000 cd m^{-2}.

2. Gravure Printing of SY on PEDOT:PSS

2.1. The Gravure Printing Process

The gravure printing process used in the present study consists of the transfer of an ink pattern from a metal engraved printing plate onto a substrate. The different steps of the gravure printing process are schematically described in **Figure 1**. In the first instance, the excess ink is removed from the engraved printing form by a doctor blade in order to fill the gravure cells with ink (Figure 1a). In the second step, the substrate, which is mounted on a rotating cylinder, is pressed against the plate and the ink is transferred to the substrate (Figure 1b). During this step the ink transfer process is frequently affected by ribbing

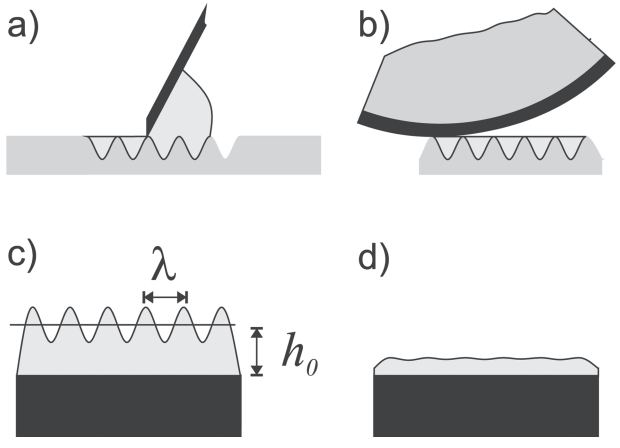

Figure 1. Schematic representation of the gravure printing process. a) Removal of the excess ink by a doctor blade and filling of the gravure cells and b) ink transfer from the gravure plate onto the substrate. c) Stabilization of the transferred ink and d) formation after evaporation of the solvent.

instabilities in the printing direction. At the final stage two competing processes will take place: surface leveling due to surface tension, and drying dictated by the evaporation rate of the solvent. If the drying time of the film is long enough, the formation of a closed and homogeneous film will take place as schematically shown in Figure 1c,d.

For the purpose of studying the gravure printing process of SY on PEDOT:PSS coated poly(ethylene terephthalate) (PET) substrates, three different concentrations of SY (5.0, 8.5, and 10.0 g L^{-1}) were prepared while systematically changing the volume fraction of benzothiazole in toluene from 0% to 40%.

2.2. Ink Surface Tension and Contact Angle

The adequate wetting of the ink on the substrate is one of the main conditions for enabling homogeneous film formation and is determined by the surface tension of the ink and the surface energy of the substrate (i.e., contact angle). Depending on the wetting properties of the ink to the printing form and the substrate theoretically up to 90% of the ink in a single gravure cell might be transferred to the substrate.[13] After the ink splitting process, the fluid surface must undergo a leveling process driven by its surface tension. As film thicknesses reduce to less than 100 nm, intra-liquid Van der Waals forces affect film stability and in some cases may favor the formation of holes by so-called "spinodal dewetting".[9] These film defects are related to laminar thin film dynamics of initially homogeneous layers. Therefore, they should be clearly separated from the fingering instabilities caused by the moving contact lines in the printing nip, which will be discussed later on.

We used the pendant drop method to determine the surface tension of the fluids. The results of the measurements are shown in **Figure 2**. A slight increase of surface tension from 28 mN m^{-1} to 36 mN m^{-1} with increasing content of benzothiazole was observed. The calculated values for the mean surface tension of toluene:benzothiazole mixtures without SY are shown as a dashed line in the top panel of Figure 2. These values were estimated from the linear interpolation of the experimentally determined surface tension of toluene (28.34 ± 0.47 mN m^{-1}) and benzothiazole (46.04 ± 0.53 mN m^{-1}). It was found that of the measured surface tension of the SY inks agrees with the calculated values of the pure solvent mixtures within a deviation of ≈1%. Hence, the magnitude of the total surface tension is mainly influenced by the ratio of the solvents since the addition of SY has little impact on the total surface tension of the fluids.

The contact angles of the different fluids to the substrate PEDOT:PSS were measured by the sessile drop method. Taking into account the behavior of the total surface tension, we would expect the contact angle to increase with higher content of benzothiazole (i.e., higher surface tension), however the results exhibited the opposite trend as depicted in the lower panel of Figure 2. According to Owens, Wendt, Rabel, and Kaelble the surface tension can be split into two additive components correspondent to polar and disperse based interactions.[14] The measured polar components of the pure solvents resulted in values below 3 mN m^{-1}. Consequently, the solvents interact with the PEDOT:PSS substrate mainly through disperse interactions

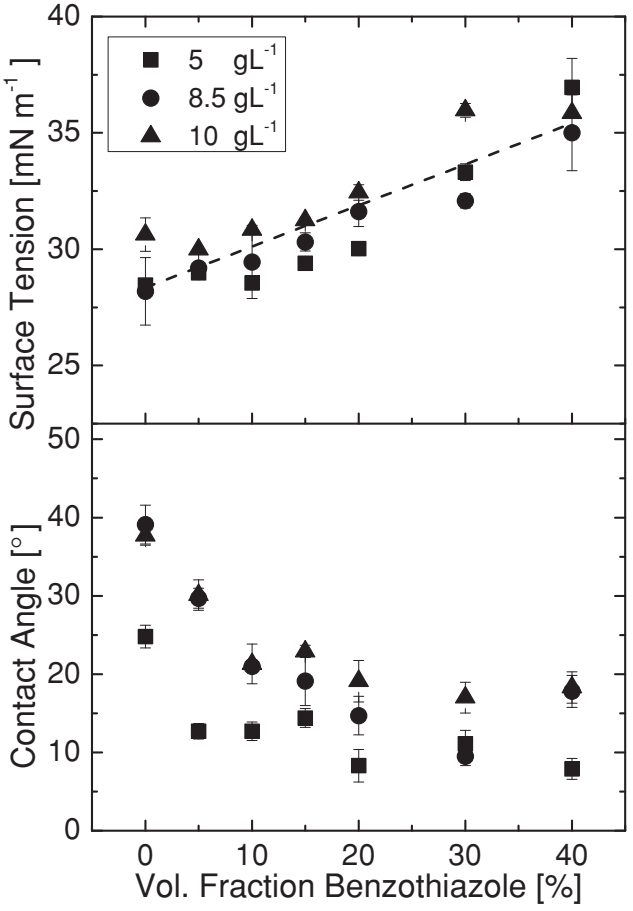

Figure 2. Surface tension and contact angle to the PEDOT:PSS surface as a function of the volume fraction of benzothiazole for the three different SY concentrations. The dashed line in the top panel represents the calculated values for the mean surface tension of toluene and benzothiazole mixtures without SY.

and cannot be responsible for the strong decrease in the contact angles. In addition, the contact angle of pure toluene and benzothiazole on the substrate was found to be 2.9° ± 0.43°. This value rises to 28.46° ± 0.24° by adding only 5 g L^{-1} SY indicating a dominant influence of the polymer, SY, on the contact angles of the ink formulations on the substrate.

2.3. Ink Viscosity

During the course of the printing process the ink is subjected to different regimes of shear forces of which the doctor blade process is the strongest. The applied shear force has an impact on the viscosity of the fluid and as a consequence influences the cell filling and ink transfer processes.[15] An overview of the dependence of the viscosity on the shear rate for the different SY formulations is presented in **Figure 3**. For the formulations prepared at a concentration of 5.0 g L^{-1} of SY for different solvent volume ratios (Figure 3a) the viscosity varies within the range of 10 mPa s to 35 mPa s at shear rates between 0.5 s^{-1} and 1000 s^{-1}. In contrast, the viscosity of the formulations

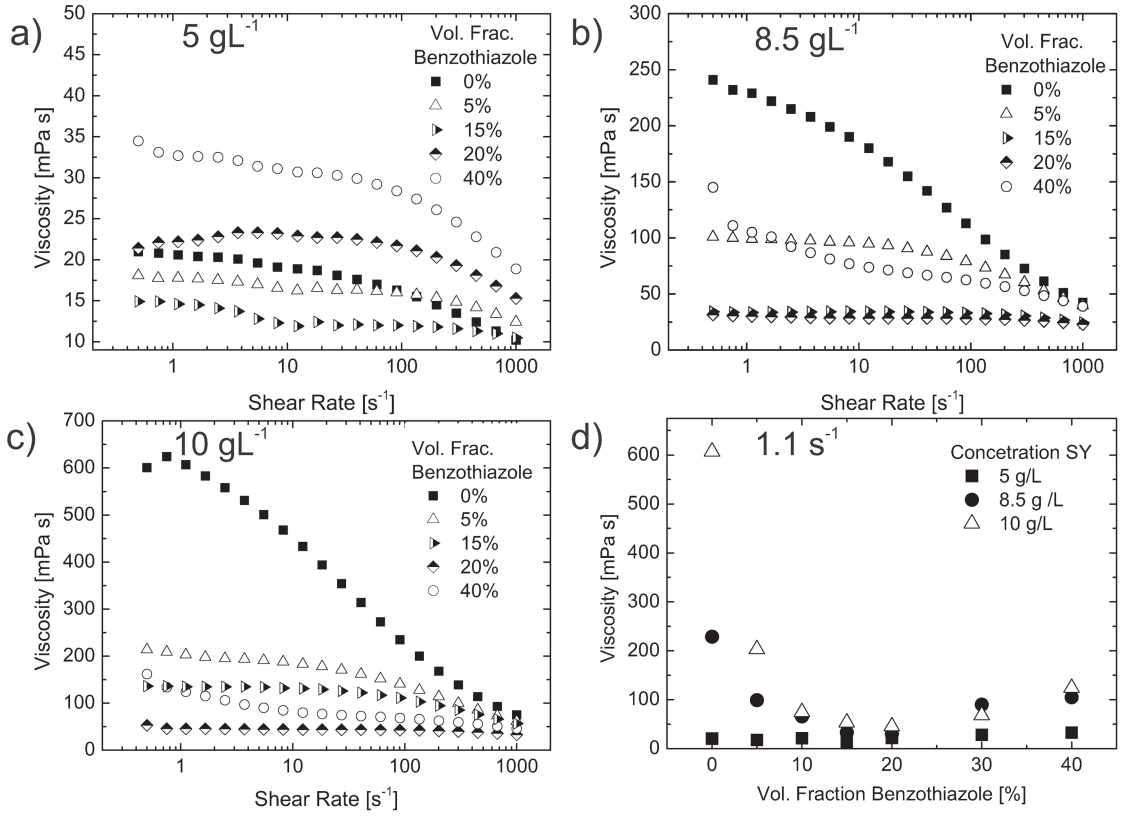

Figure 3. a–c) Viscosity of the ink formulations as a function of shear rate for 5, 8.5, and 10 g L^{-1}, respectively. d) Ink viscosity as a function of benzothiazole volume fraction at a shear rate of 1.1 s^{-1}.

prepared at 8.5 and 10.0 g L^{-1} exhibited a change of up to an order of magnitude for the same range parameters. It is worth noting that all formulations undergo shear thinning of the viscosity although a much less pronounced dependency is exhibited by the formulations prepared from mixtures between 15% and 20% of benzothiazole. Formulations with solvent ratios outside this regime exhibit a strong nonlinear relation to the shear rate (i.e., non-Newtonian behavior). Due to the shear thinning of the viscosity, it is expected that all formulations will behave in a similar fashion during the doctor blade process and the ink transfer where shear forces are maximized. On the contrary, since we did not measure a considerable shear memory effect (thixotropy) for any formulation, the behavior of the fluid at the surface leveling step will vary in correlation to its viscosity at low shear rates (see Figure 3a–c). Figure 3d shows the magnitude of the viscosity at shear rate of 1.11 s^{-1}. At around 20% volume fraction of benzothiazole, the existence of a local minimum is observed independently of the SY content. The lower viscosity of these formulations at low shear rates is expected to induce favorable film conformation during the drying process.

2.4. Printing Outcome and Film Leveling Time

A chart composed of contrast enhanced optical microscope images of the 2.25 cm^2 printing fields and its corresponding fast-Fourier transform (FFT) is presented in **Figure 4**. The FFT diagrams are a representation of the distribution of the pixel intensity in the optical microscope image, and the possible periodicity that results from the variation of the film thickness in the printed film. The FFT diagrams can be used to qualitatively compare the homogeneity of the films since a modulation in the microscope image would yield a pattern in the FFT image. In contrast, an ideal homogeneous layer would be represented as a single dot in the center of the diagram. For all toluene-only solutions a film thickness modulation along the printed direction is observed and it is translated as a horizontal pattern in the FFT image. Subsequent addition of benzothiazole creates a window of compositions where the surface modulation is reduced as corroborated by FFT diagrams. The best film homogeneity is observed for the fields with benzothiazole vol. fractions close to 15% and 20%. Further increase in benzothiazole to volume ratios close to 40% disfavors homogeneous film conformation again and shows similar ribbing structure as for small volume ratios as well.

The formation of the present layer thickness undulations during the printing processes (also called viscous fingering or Saffman-Taylor instability) are a common phenomenon in coating and printing applications and have been extensively studied.[16,17] The onset for the instability is a receding fluid meniscus confined between two walls with small distance as described and analyzed in the model geometry of a Hele-Shaw cell.[18] In the present system, the latter is described by the fluid splitting between the gravure cylinder and the substrate in

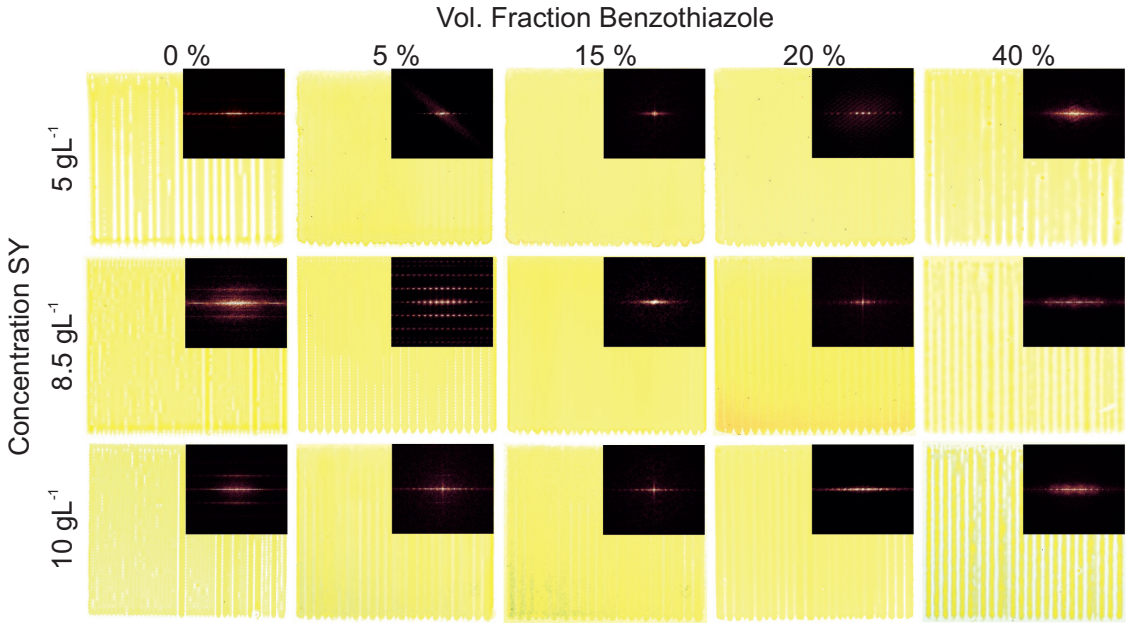

Figure 4. Contrast-enhanced optical microscope images of the gravure printed SY films prepared at different concentrations and solvent mixtures. Insets: FFT representation of the corresponding printing field image. Each printing field is 2.25 cm^2.

the printing nip. Due to its low viscosity, the printing fluid is not only deposited from the gravure cells but it also wets the walls, which supports the formation of a continuous meniscus when the printing form is lifted from the substrate. At critical system and fluid parameters, the lamella-like meniscus in the nip favors a disturbed fluid surface rather than a straight one. This results in a growing periodic modulation of the film surface along the printing direction, excluding Marangoni forces as the origin of the fingering. In other words, it is dependent on hydrodynamic instabilities in the printing nip (i.e., Saffman-Taylor instability) rather than on surface tension gradients.[9] The predominant wavelength of the patterns is a function of the cell depth, printing speed, viscosity, surface tension and distance from the fluid meniscus nip to the point where the gravure plate touches the substrate. More details on the relationship between the important parameters and numerical simulations based on the Lattice-Boltzmann method applied to the fingering phenomena in printing processes are given by Voss.[19] Engineering of the gravure cells and optimization of the printing speed could also help to improve the printing outcome.[20] The characteristic leveling time (τ_{lev}) of the patterns created during the ink transfer process is correlated to the thin film parameters through the expression presented in Equation 1, where η, σ_T, h_0, and λ, respectively, represent the viscosity, total surface tension, wet film thickness, and period of the thickness modulation of the film (see also Figure 1c).[21,22]

$$\tau_{lev} = \frac{3\eta\lambda^4}{16\pi^4\sigma_T h_0^3} \quad (1)$$

The derivation of this characteristic time is based on a linear stability analysis of the Navier-Stokes equations neglecting evaporation and assuming constant viscosity and constant surface tension.[22] It is important to note that the leveling time depends linear on surface tension and viscosity, cubed on the wet film thickness and to the power of four on the wavelength of undulation.

In order to obtain a printed layer with a homogeneous thickness, τ_{lev} should be smaller than the critical "freezing" time τ_c, at which the film has become too viscous and lost its mobility due to solvent evaporation. For a SY concentration of 15 g L^{-1} at 20% volume fraction of benzothiazole the viscosity at low shear rates increases by an order of magnitude reaching values of ≈400 mPa s. Therefore, we define τ_c as the necessary time to achieve a concentration of 15 g L^{-1} assuring that at this point the properties of the fluid will not allow for favorable film leveling during the time scale of the drying process. Assuming a constant surface area and therefore a constant evaporation rate, we can estimate τ_c as the corresponding fraction of the experimentally determined drying time. The linear dependency of the drying time with respect to the volume fraction of benzothiazole averaged for all SY concentrations is shown in **Figure 5**a. By using of Equation 1, we calculated τ_{lev} and plotted it in Figure 5b–d as a function of the solvent ratio for 5.0, 8.5, and 10.0 g L^{-1}, respectively. The wet film height, h_0, was estimated from the solid film thickness and the SY concentration. The average film thicknesses as measured by profilometry were found to be 36 nm ± 4 nm, 77 nm ± 8 nm, and 98 nm ± 8 nm for the formulations with 5.0, 8.5, and 10.0 g L^{-1} of SY, respectively. The modulation wavelength, λ, was determined from the profilometry measurements and optical microscopy images and had a constant magnitude of ≈0.7 mm for all printing results. The viscosity values at a low shear rate (1.11 s^{-1}) were used for the calculation.

According to Equation 1, higher surface tension promotes faster leveling. The change of surface tension as a function

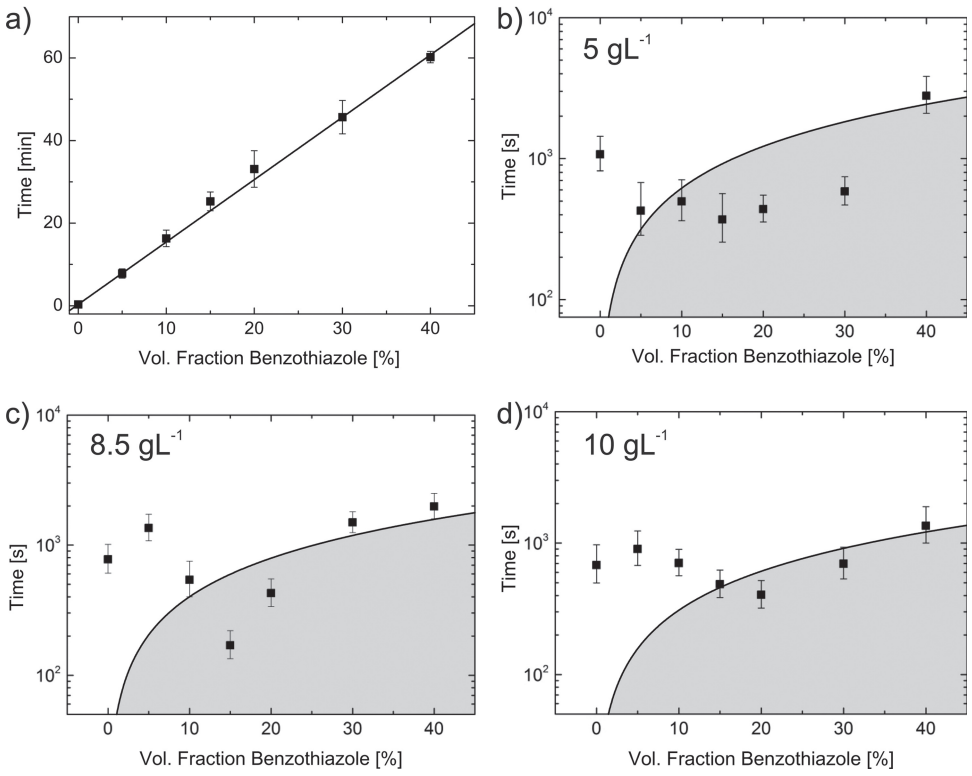

Figure 5. (a) Measured film drying time. The solid line represents a linear fit to the experimental data. b–d) Comparison of the critical freezing time (solid line) and the calculated leveling time (filled squares) as a function of the benzothiazole volume fraction for SY concentrations of 5, 8.5, and 10 10 g L^{-1}, respectively.

of vol. fraction of benzothiazole or the content of SY is small compared to the change in the viscosity (see Figure 2). In addition, the modulation wavelength and the film height were assumed to stay constant. Therefore, the magnitude of τ_{lev} will be mainly dictated by the viscosity behavior. Even though the contact angles are not included in the present model for τ_{lev}, this variable is important since smaller angle results in faster spreading of the ink. Hence, it should be small enough for allowing the finger-like structures to coalesce to a closed liquid surface. According to the large contact angles measured for the printed fields of mixtures of 0 and 5% volume fraction of benzothiazole, liquid spreading is expected to be lower than for fields of higher vol. fractions. Therefore, the line structure that is formed in the printing nip might be immobile due to high contact angles of the ink on the substrate.

We observed that the minimum values of the leveling time for inks at 15% and 20% volume fraction of benzothiazole are considerably below the critical drying time ($\tau_{lev} < \tau_c$), which is in agreement with the printing outcome presented in Figure 4. The origin of the predominant minima shown in Figure 5b–d, can be mainly correlated to the behavior of the benzothiazole dependent viscosity. Equation 1 states a linear relation of the leveling time and the viscosity. Therefore, we expect the minima of the viscosity at 15% volume fraction benzothiazole for 5.0 and 8.5 g L^{-1} of SY and 20% for 10 g L^{-1} of SY (compare Figure 3d) to match the most homogeneous printing outcome. Indeed, the microscope images shown in Figure 4 demonstrate that the utilized model can accurately describe the gravure printing process for a given printing speed and gravure cell design.

3. Gravure Printed OLEDs

Flexible OLEDs were prepared on pre-structured indium tin oxide (ITO)/PET substrates. A gravure printed PEDOT:PSS layer was utilized to lower the ITO work function and assist hole injection. Solvent mixtures of 5 and 15% volume fraction of benzothiazole in toluene were used to dissolve SY at a concentration of 8.5 g L^{-1}. The gravure printed SY emitting layer yielded a nominal thickness of ≈75 nm. Finally, a Ca/Al layer was thermally evaporated to be used as a cathode. Optical images of the gravure printed OLEDs under operation are presented in **Figure 6**. The device prepared using the solution with 5% volume fraction of benzothiazole shows a pattern of parallel lines that illustrate the non-uniformity of the layers (see Figure 6a). The modulation of the active layer thickness causes an inhomogeneity in the electric field and thus zones of the active layer where the emission point is reached at a higher voltage. The use of a homogeneous film printed for the 15% volume fraction benzothiazole formulation results in a considerable improvement in the luminescence uniformity over the whole device area as seen from Figure 6b. Figure 6c shows the electro-optical properties of the two devices. As expected, the device prepared with an inhomogeneous SY layer delivers a poorer performance. The lower current, higher threshold

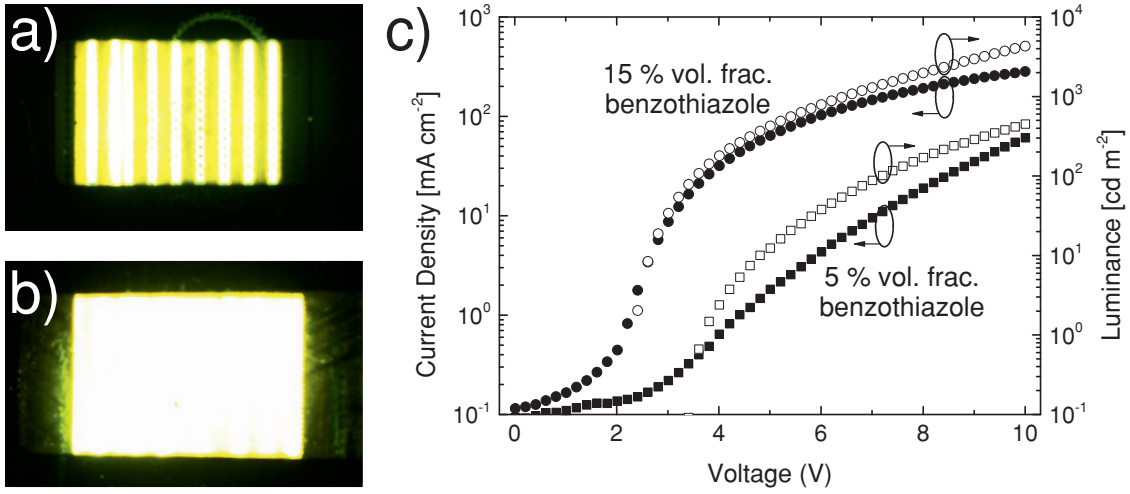

Figure 6. Optical images of gravure printed SY based OLEDs under operation. The devices were prepared with formulations containing a) 5% and b) 20% volume fractions of benzothiazole using a SY concentration of 8.5 g L^{-1}. c) Current density–voltage (*I–V*) and luminance characteristics of the fabricated OLEDs.

voltage, and lower luminance on this device are a consequence of the non-uniform electric field and smaller luminescent area. Typically, the luminous efficiencies obtained for the 15% volume benzothiazole devices (≈2 cd A^{-1}) were only two times larger than for the 5% even though the luminance presented one order of magnitude difference. These relative low efficiency values suggest that, due to its high boiling point, benzothiazole could still be present in the film and have an adverse effect over the device performance. This effect should be studied in the future in order to optimize the device fabrication. The presented flexible OLEDs achieve luminance values close to 5000 cd m^{-2} without any optimization or post-treatment demonstrating the potential use of gravure printing for fabrication of high performance devices.

4. Conclusions

A two solvent mixture consisting of toluene and benzothiazole was used to study and successfully print SY on PEDOT:PSS by gravure printing. It was observed that SY-toluene formulations yield thin films with a strong thickness modulation caused by instabilities during the ink transfer process and fast drying. Upon addition of benzothiazole, film drying time increases, however, favorable film conformation is only permitted at benzothiazole volume fractions close to 15% and 20%. At these solvent ratios viscosity is minimized and the formulation behaves as a Newtonian fluid, promoting the shortest demodulation time of the printed wet layer films according to the applied model of leveling. The estimated demodulation time of the film was in agreement with the experimental results. When comparing the demodulation time to the critical "freezing" time of the film, we were able to identify the conditions at which optimal film morphology is obtained. With the knowledge obtained from the printing process, flexible OLEDs with luminance of up to 5000 cd m^{-2} were fabricated from the optimized formulation. Therefore, it is hereby shown that the gravure printing technique can be used as a tool for the production of organic optoelectronic devices. Moreover, it is shown that the interplay between surface tension, viscosity, and drying time must be considered carefully in order to improve the quality and reproducibility of organic thin-film devices fabricated by gravure printing.

5. Experimental Section

Printing Tests Sample Preparation: SY (PDY-132 LIVILUX, Merck) was dissolved for several hours in solvent mixtures of toluene and benzothiazole at different volume ratios at a concentration of 5, 8.5 and 10 g L^{-1}. The different formulations were printed on PEDOT:PSS (Clevios) covered PET substrates using a RK gravure printing proofer with a field size of 2.25 cm^2 at a speed of ≈1 m s^{-1}. The cell volume per area of the gravure plate was 14 mL m^{-2} with 54 lines per cm. The PET substrates were covered with PEDOT:PSS using a similar formulation as reported in ref. [6] with help of a Zehnter ZAA 2300 film applicator.

Surface Tension Measurements: The surface tension and contact angle measurements were performed with a Krüss DSA100 at 23 °C. The pendent drop method was used to determine the surface tension of the liquids. To reduce the effect of fast solvent evaporation of toluene during the drop shape acquisition, several drops were created, slow enough such that gravity and surface tension could balance and fast enough for evaporation to be negligible. Contact angles were captured with a viewing angle of 2° off the horizontal of the printing inks on the PEDOT:PSS/ITO/PET substrates.

Viscosity Measurements: Viscosity as a function of shear rate was measured at 23 °C using a volume of 1 mL using the cone-plate geometry on a HAAKE MARS rheometer.

OLED Fabrication and Characterization: OLEDs were prepared on pre-structured ITO/PET substrates previously treated by oxygen plasma. A layer of PEDOT:PSS (≈60 nm) was gravure printed in top of the ITO pattern. Subsequently the SY formulation was gravure printed. Finally, a Ca (20 nm)/Al (100 nm) cathode was vacuum deposited through a shadow mask to produce four devices (6 mm × 4 mm) per printing field. OLED characterization was performed using a calibrated BOTEST system.

Acknowledgements

The authors are thankful to M. Müller-Zander for technical support and A. Rupprecht for fruitful discussion. They acknowledge the German Federal Ministry of Education and Research (BMBF) for the financial support: FKZ13N10760 and FKZ 13N12127.

Received: October 2, 2012
Published online: February 7, 2013

[1] a) J. R. Sheats, *J. Mater. Res.* **2004**, *19*, 1974; b) S. R. Forrest, *Nature* **2004**, *428*, 911; c) S. Logothetidis, *Mater. Sci. Eng. B* **2008**, *152*, 96; d) F. C. Krebs, T. Tromholt, M. Jørgensen, *Nanoscale* **2010**, *2*, 873.

[2] a) R. H. Friend, R. W. Gymer, A. B. Holmes, J. H. Burroughes, R. N. Marks, C. Taliani, D. D. C. Bradley, D. A. Dos Santos, J. L. Bredas, M. Lögdlund, W. R. Salaneck, *Nature* **1999**, *397*, 121; b) M. Riede, T. Mueller, W. Tress, R. Schueppel, K. Leo, *Nanotechnology* **2008**, *19*, 424001; c) H. Sirringhaus, *Adv. Mater.* **2005**, *17*, 2411; d) S. Günes, H. Neugebauer, N. S. Sariciftci, *Chem. Rev.* **2007**, *107*, 1324.

[3] a) A. Facchetti, *Mater. Today* **2007**, *10*, 28; b) M. A. Green, K. Emery, Y. Hishikawa, W. Warta, E. D. Dunlop, *Prog. Photovolt: Res. Appl.* **2012**, *20*, 12.

[4] a) M. Kittila, J. Hagberg, E. Jakku, S. Leppavuori, *IEEE Trans. Electron. Packag. Manuf.* **2004**, *27*, 109; b) M. Pudas, *J. Eur. Ceram. Soc.* **2004**, *24*, 2943; c) J. Jo, J.-S. Yu, T.-M. Lee, D.-S. Kim, *Jpn. J. Appl. Phys.* **2009**, *48*, 04C181; d) D. Sung, A. de la Fuente Vornbrock, V. Subramanian, *IEEE Trans. Comp. Packag. Technol.* **2010**, *33*, 105.

[5] a) M. M. Voigt, R. C. I. Mackenzie, C. P.Yau, P. Atienzar, J. Dane, P. E. Keivanidis, D. D. C. Bradley, J. Nelson, *Sol. Energy Mater. Sol. Cells* **2011**, *95*, 731; b) H. Kang, R. Kitsomboonloha, J. Jang, V. Subramanian, *Adv. Mater.* **2012**, *22*, 3065; c) A. de la Fuente Vornbrock, D. Sung, H. Kang, R. Kitsomboonloha, V. Subramanian, *Org. Electron.* **2010**,*11*, 2073; d) A. Kim, H. Lee, J. Lee, S. M. Cho, H. Chae, *J. Nanosci. Nanotechnol.* **2011**, *11*, 546; e) P. Kopola, T. Aernouts, R. Sliz, S. Guillerez, M. Ylikunnari, D. Cheyns, M. Välimäki, M. Tuomikoski, J. Hast, G. Jabbour, R. Myllylä, A. Maaninen, *Sol. Energy Mater. Sol. Cells* **2011**, *95*, 1344; f) F. C. Krebs, *Sol. Energ. Mat. Sol. C* **2009**, *93*, 394.

[6] D.-Y. Chung, J. Huang, D. D. C. Bradley, A. J. Campbell, *Org. Electron.* **2010**, *11*, 1088.

[7] M. M. Voigt, A. Guite, D.-Y. Chung, R. U. A. Khan, A. J. Campbell, D. D. C. Bradley, F. Meng, J. H. G. Steinke, S. Tierney, I. McCulloch, H. Penxten, L. Lutsen, O. Douheret, J. Manca, U. Brokmann, K. Sönnichsen, D. Hülsenberg, W. Bock, C. Barron, N. Blanckaert, S. Springer, J. Grupp, A. Mosley, *Adv. Funct. Mater.* **2010**, *20*, 239.

[8] A. Kim, H. Lee, C. Ryu, S. M. Cho, H. Chae, *J. Nanosci, Nanotechnology* **2010**, *5*, 3326.

[9] N. Bornemann, H. M. Sauer, E. Dörsam, *J. Imaging Sci. Technol.* **2011**, *55*, 040201.

[10] a) F. Zhang, K. G. Jespersen, C. Björström, M. Svensson, M. R. Andersson, V. Sundström, K. Magnusson, E. Moons, A. Yartsev, O. Inganäs, *Adv. Funct. Mater.* **2006**, *16*, 667; b) H. Hoppe, N.S. Sariciftci, *J. Mater. Chem.* **2006**, *16*, 45; c) L. G. Kaake, G. C. Welch, D. Moses, G. C. Bazan, A. J. Heeger, *J. Phys. Chem. Lett.* **2012**, *3*, 1253; d) T. Salim, L. H. Wong, B. Bräuer, R. Kukreja, Y. L. Foo, Z. Bao, Y. M. Lam, *J. Mater. Chem.* **2011**, *21*, 242; e) D. K. Hwang, C. Fuentes-Hernandez, J. D. Berrigan, Y. Fang, J. Kim, W. J. Potscavage Jr., H. Cheun, K. H. Sandhage, B. Kippelen, *J. Mater. Chem.* **2012**, *22*, 5531.

[11] a) P. Esena, C. Riccardi, S. Zanini, M. Tontini, G. Poletti, F. Orsini, *Surf. Coat. Technol.* **2005**, *200*, 664; b) S. Besbes, H. B. Ouada, J. Davenas, L. Ponsonnet, N. Jaffrezic, P. Alcouffe, *Mater. Sci. Eng. C* **2006**, *26*, 505; c) S. Archambeau, I. Seguy, P. Jolinat, J. Farenc, P. Destruel, T. Nguyen, H. Bock, E. Grelet, *Appl. Surf. Sci.* **2006**, *253*, 2078; d) D. Hegemann, H. Brunner, C. Oehr, *Nucl. Instrum. Meth. B* **2003**, *208*, 281.

[12] H. Spreitzer, H. Becker, E. Kluge, W. Kreuder, H. Schenk, R. Demandt, H. Schoo, *Adv. Mater.* **1998**, *10*, 1340.

[13] F. Ghadiri, D. H. Ahmed, H. J. Sung, E. Shirani, *Int. J. Heat Fluid Flow* **2011**, *32*, 308.

[14] a) D. Y. Kwok, A.W. Neumann, *Adv. Colloid Interface Sci.* **1999**, *81*, 167; b) D. K. Owens, R. C. Wendt, *J. Appl. Polym. Sci.* **1969**, *13*, 1741.

[15] S. Elsayad, F. Morsy, S. El-Sherbiny, E. Abdou, *Pigm. Resin Technol.* **2002**, *31*, 234.

[16] a) J. V. Maher, *Phys. Rev. Lett.* **1985**, *54*,1498; b) S. K. Wilson, *IMA J. Appl. Math.* **1993**, *10*, 149.

[17] K. Reuter, H. Kempa, N. Brandt, M. Bartzsch, A. C. Huebler, *Prog. Org. Coat.* **2007**, *58*, 312.

[18] P. G. Saffman, G. I. Taylor, *Proc. R. Soc.* **1958**, *A245*, 312.

[19] C. Voss, *PhD thesis*, Bergische Universität Wuppertal, Germany **2002**.

[20] J. J. Michels, S. H. P. M. de Winter, L. H. G. Symonds, *Org. Electron.* **2009**, *10*, 1495.

[21] N. Bornemann, H. M. Sauer, E. Dörsam, *Large-area, Organic & Printed Electronics Convention (LOPE-C)*, Organic and Printed Electronics Association, Frankfurt, Germany **2010**, p. 138.

[22] S. Orchard, *Appl. Sci. Res.* **1963**, *11*, 451.